



**HAL**  
open science

## Rate Constants of the CN plus Toluene Reaction from 15 to 294 K and Interstellar Implications

Joseph P. Messinger, Divita Gupta, Ilsa R. Cooke, Mitchio Okumura, Ian R. Sims

► **To cite this version:**

Joseph P. Messinger, Divita Gupta, Ilsa R. Cooke, Mitchio Okumura, Ian R. Sims. Rate Constants of the CN plus Toluene Reaction from 15 to 294 K and Interstellar Implications. *Journal of Physical Chemistry A*, 2020, 124 (39), pp.7950-7958. 10.1021/acs.jpca.0c06900 . hal-02996160

**HAL Id: hal-02996160**

**<https://hal.science/hal-02996160>**

Submitted on 16 Nov 2020

**HAL** is a multi-disciplinary open access archive for the deposit and dissemination of scientific research documents, whether they are published or not. The documents may come from teaching and research institutions in France or abroad, or from public or private research centers.

L'archive ouverte pluridisciplinaire **HAL**, est destinée au dépôt et à la diffusion de documents scientifiques de niveau recherche, publiés ou non, émanant des établissements d'enseignement et de recherche français ou étrangers, des laboratoires publics ou privés.

1  
2  
3  
4  
5  
6  
7  
8  
9  
10  
11  
12  
13  
14  
15  
16  
17  
18  
19  
20  
21  
22  
23  
24  
25  
26  
27  
28  
29  
30  
31  
32  
33  
34  
35  
36  
37  
38  
39  
40  
41  
42  
43  
44  
45  
46  
47  
48  
49  
50  
51  
52  
53  
54  
55  
56  
57  
58  
59  
60

# Rate Constants of the CN + Toluene Reaction from 15 – 294 K and Interstellar Implications

Joseph P. Messinger,<sup>a,b</sup> Divita Gupta,<sup>b</sup> Ilsa R. Cooke,<sup>b</sup> Mitchio Okumura,<sup>a,\*</sup> Ian R. Sims<sup>b,\*</sup>

<sup>a</sup> Arthur Amos Noyes Laboratory of Chemical Physics, Division of Chemistry and Chemical Engineering, California Institute of Technology, 1200 East California Boulevard, Pasadena, California 91125, United States

<sup>b</sup> Univ Rennes, CNRS, IPR (Institut de Physique de Rennes) - UMR 6251, F-35000 Rennes, France

\*Corresponding authors: MO: mo@caltech.edu, IRS: ian.sims@univ-rennes1.fr

1  
2  
3 ABSTRACT  
4  
5  
6

7 CN is known for its fast reactions with hydrocarbons at low temperatures, but relatively few studies  
8 have focused on the reactions between CN and aromatic molecules. The recent detection of  
9 benzonitrile in the interstellar medium, believed to be produced by the reaction of CN and benzene,  
10 has ignited interest in studying these reactions. Here, we report rate constants of the CN + toluene  
11 ( $C_7H_8$ ) reaction between 15 and 294 K using a CRESU (*Cinétique de Réaction en Ecoulement*  
12 *Supersonique Uniforme*; reaction kinetics in uniform supersonic flow) apparatus coupled with the  
13 pulsed laser photolysis – laser induced fluorescence (PLP-LIF) technique. We also present the  
14 stationary points on the potential energy surface of this reaction to study the available reaction  
15 pathways. We find the rate constant does not change over this temperature range, with an average  
16 value of  $(4.1 \pm 0.2) \times 10^{-10} \text{ cm}^3 \text{ s}^{-1}$ , which is notably faster than the only previous measurement at  
17 105 K. While the reason for this disagreement is unknown, we discuss the possibility that it is  
18 related to enhanced multiphoton effects in the previous work.  
19  
20  
21  
22  
23  
24  
25  
26  
27  
28  
29  
30  
31  
32  
33  
34  
35  
36  
37  
38  
39  
40  
41  
42  
43  
44  
45  
46  
47  
48  
49  
50  
51  
52  
53  
54  
55  
56  
57  
58  
59  
60

## Introduction

The CN radical has long been known to be abundant in the interstellar medium (ISM), where it was first detected in 1940s,<sup>1-2</sup> and in the atmosphere of Titan, where it leads to the formation of nitrile compounds, including  $C_2H_3CN$  and  $HC_3N$ .<sup>3-5</sup> At the low temperatures found in these environments, reactions between CN and other compounds are known to have fast rate constants, on the order of  $10^{-10} \text{ cm}^3 \text{ s}^{-1}$ , and thus must be included in gas-phase models. Reactions between CN and hydrocarbons are among the fastest of these rates, and proceed through either an abstraction or an addition mechanism.<sup>6</sup> A number of cyano-containing molecules linked to these reactions have been found in ISM, including molecules as large as  $HC_9N$  and  $(CH_3)_2CHCN$ .<sup>7,8</sup> On Titan, the photolysis of these nitrile compounds formed from CN reactions may contribute to the formation of particulate matter.<sup>9</sup>

On Titan, toluene has been detected in the upper atmosphere by the Cassini Ion and Neutral Mass Spectrometer,<sup>10</sup> and while it is currently undetected in the lower atmosphere, models suggest it has a high abundance there as a product of the fast association reaction between  $C_6H_5$  and  $CH_3$ .<sup>11</sup> In addition to benzene and toluene, a large number of specific polycyclic aromatic hydrocarbons (PAHs) have also been identified.<sup>12</sup> These PAHs are believed to form from smaller aromatic compounds and to be an important component of the thick haze in Titan's atmosphere.<sup>13</sup>

On the other hand, very few specific aromatic molecules have been directly detected in the ISM, in part due to their low dipole moments making them difficult to observe by radio astronomy. Benzene has been observed through infrared observations,<sup>14</sup> and PAHs are widely believed to be abundant in the ISM owing to observations of the strong infrared bands characteristic of these molecules, but the broad, overlapping nature of these bands has precluded the identification of

1  
2  
3 specific PAHs.<sup>15</sup> Despite this lack of definitive identifications, PAHs are believed to hold a large  
4  
5 fraction of carbon in the ISM,<sup>16-17</sup> and so their formation has been the subject of extensive study.<sup>18-</sup>  
6

7  
8 <sup>20</sup> The formation of the first aromatic ring is believed to be the rate limiting step in PAH  
9  
10 formation,<sup>21</sup> and so understanding the chemistry of these monocyclic aromatic compounds is  
11  
12 necessary.  
13

14  
15 The recent detection of benzonitrile in the ISM<sup>22</sup> has suggested a new route for understanding  
16  
17 aromatic formation. Benzonitrile is believed to be the product from the CN + benzene reaction,  
18  
19 which we have recently shown to be fast at low temperatures,<sup>23</sup> with a rate constant of  $(4.4 \pm 0.2)$   
20  
21  $\times 10^{-10} \text{ cm}^3 \text{ s}^{-1}$  over the 15 – 294 K range, in good agreement with earlier work by Trevitt et al.  
22  
23 down to 105 K.<sup>24</sup> Observations of benzonitrile therefore can be used as a proxy for the abundance  
24  
25 of benzene. Other aromatic nitriles may also serve as proxies for undetected aromatic compounds  
26  
27 in the ISM, as the addition of the cyano moiety gives these compounds large dipole moments and  
28  
29 makes them visible to radio astronomy. The identification of additional specific aromatic  
30  
31 compounds would significantly constrain models of PAH formation in the ISM.  
32  
33  
34

35  
36  
37 However, little is known about the reaction of CN with other aromatic molecules and whether  
38  
39 these reactions also result in the formation of nitrile compounds. Only one rate constant for the  
40  
41 reaction between CN and toluene, one of the simplest aromatics, has been measured, by Trevitt et  
42  
43 al.<sup>24</sup> They studied this reaction at 105 K and found a rate constant of  $(1.3 \pm 0.3) \times 10^{-10} \text{ cm}^3 \text{ s}^{-1}$  using  
44  
45 pulsed laser photolysis – laser induced fluorescence (PLP-LIF) measurements in conjunction with  
46  
47 a pulsed Laval nozzle. This rate constant is a factor of 3 lower than the rate constants measured  
48  
49 for the CN + benzene reaction measured in the same study as well as our own,<sup>23,24</sup> suggesting that  
50  
51 the structure of aromatic molecules can play a large role in the reaction rates. Furthermore, they  
52  
53 observed non-exponential decays of CN at room temperature in the presence of toluene and were  
54  
55  
56  
57  
58  
59  
60

1  
2  
3 therefore unable to measure a rate constant, in contrast with their measurements of benzene under  
4  
5 the same conditions. They suggested that this could be due to dissociation of the products back to  
6  
7 the CN + toluene reactants, and that further studies would be necessary to better understand these  
8  
9 results.  
10

11  
12  
13 The difference between the rate constants of the CN + benzene and CN + toluene reactions would  
14  
15 seem to suggest that the structure of an aromatic compound can play a large role in the reaction  
16  
17 dynamics. This makes it questionable whether nitrile compounds may be formed from the  
18  
19 reactions of CN with larger, more complex aromatic compounds, and it is essential to verify the  
20  
21 reliability of using cyano-substituted compounds as a proxy for larger aromatic species. To that  
22  
23 end, we have conducted measurements of the CN + toluene rate constant between 16 and 294 K  
24  
25 to gain further insight into this reaction, especially at the low temperatures relevant to the ISM and  
26  
27 Titan. Furthermore, we have computed stationary points on the potential energy surface (PES) of  
28  
29 the CN + toluene reaction to better understand the possible products and mechanism of this  
30  
31 reaction.  
32  
33  
34  
35  
36

### 37 **Experimental Section**

38  
39  
40 Rate constants were determined using the PLP-LIF technique. Temperatures down to 15 K were  
41  
42 achieved using the CRESU technique (*Cinétique de Réaction en Ecoulement Supersonique*  
43  
44 *Uniforme*; reaction kinetics in uniform supersonic flow), which has been described in detail  
45  
46 previously.<sup>6,25-26</sup> Briefly, toluene (Sigma Aldrich, 99.9%) was introduced into the gas flow with a  
47  
48 Controlled Evaporation and Mixing system (Bronkhorst CEM), as described in Gupta et al.<sup>27</sup> The  
49  
50 toluene and ICN (Acros Organics, 98%), used as the CN precursor, were mixed in a buffer gas of  
51  
52 He (99.995%, Air Liquide), Ar (99.998%, Air Liquide) or N<sub>2</sub> (99.995%, Air Liquide), depending  
53  
54  
55  
56  
57  
58  
59  
60

1  
2  
3 on the desired CRESU conditions. Concentrations of toluene and ICN were kept < 1% of the total  
4 density in order not to affect the uniformity of the gas flow. The mixture was flowed isentropically  
5  
6 from a high pressure reservoir through specifically designed convergent-divergent Laval nozzles,  
7  
8 into a low pressure chamber to generate a uniform supersonic flow at the appropriate temperature  
9  
10 with a density of  $10^{16} - 10^{17} \text{ cm}^{-3}$ . Each nozzle was characterized with Pitot probe impact pressure  
11  
12 measurements prior to experiments to determine the temperature, density and uniformity of the  
13  
14 gas flow. For measurements at 294 K, where a supersonic expansion is not required, the pumping  
15  
16 speed was decreased such that the pressure in the reservoir and the chamber were equal, while  
17  
18 maintaining complete gas turnover for each laser shot.  
19  
20  
21  
22  
23

24  
25 CN radicals were generated by the 248 nm photolysis of ICN using a KrF excimer laser (Coherent  
26  
27 LPXPro 210) operating at 10 Hz, with a laser fluence of  $25 \text{ mJ cm}^{-2}$ . The third harmonic of a  
28  
29 Nd:YAG laser (Continuum, Powerlite Precision II), also operating at 10 Hz, was used to pump a  
30  
31 dye laser (Laser Analytical Systems, LDL 20505) containing Exalite 389 (Exciton) in 1,4-dioxane  
32  
33 (Sigma Aldrich, 99.8%) to produce  $\sim 389 \text{ nm}$  light to excite the CN  $B^2\Sigma^+ - X^2\Sigma^+ (0,0)$  transition.  
34  
35 Fluorescence was detected from the CN (0,1) transition at  $\sim 420 \text{ nm}$  by a photomultiplier tube  
36  
37 (Thorn EMI 6723) preceded by a 420 nm bandpass filter (Ealing Optics). The delay time between  
38  
39 the excimer and the Nd:YAG pump laser was varied from -5 to 200 microseconds to record the  
40  
41 time dependence of the CN signal. The LIF signal was recorded by a gated integrator for 400  
42  
43 evenly spaced points and averaged 5 times. The resulting kinetic trace was fit to an exponential  
44  
45 decay starting  $\geq 10 \mu\text{s}$  after photolysis to allow for rotational thermalization of CN.  
46  
47  
48  
49  
50

51 Kinetic measurements were taken under pseudo-first order conditions with  $[\text{toluene}] \gg [\text{CN}]$ .  
52  
53 Typical toluene concentrations were on the order of  $10^{12} - 10^{13} \text{ cm}^{-3}$ , while we estimate the CN  
54  
55 concentration to be roughly  $10^{10} \text{ cm}^{-3}$  based on the ICN concentration ( $\sim 10^{12} \text{ cm}^{-3}$ ) and 248 nm  
56  
57  
58  
59  
60

1  
2  
3 absorption cross section of  $4.7 \times 10^{-19} \text{ cm}^2$ .<sup>28</sup> More than 90% of the CN radicals from the photolysis  
4  
5 of ICN at 248 nm are in the ground vibrational state<sup>29</sup> and we do not observe any influence of the  
6  
7 relaxation of excited vibrational states on our kinetic measurements.  
8  
9

## 10 11 **Computational Details**

12  
13  
14 Investigation of possible channels for the reaction between CN and toluene, with identification of  
15  
16 all the stationary points (minima, complexes, and transition states), was done using Gaussian 09  
17  
18 software<sup>30</sup>; all included channels can be seen in Figure 1. All the species, including the reaction  
19  
20 complexes and transition states were optimized at (U)M06-2X/aug-cc-pVTZ level<sup>31-33</sup> and zero-  
21  
22 point corrected energies were calculated for each. In addition, intrinsic reaction coordinate (IRC)  
23  
24 calculations were performed at (U)M06-2X/6-311G to determine the minimum energy path that  
25  
26 the transition states followed to confirm the connection between the appropriate reactants and  
27  
28 products. Gibbs energies ( $\Delta_r G^\circ$  (298 K)) for all included channels were also calculated at (U)M06-  
29  
30 2X/aug-cc-pVTZ method. Both addition-elimination channels, leading to nitrile formation, and  
31  
32 abstraction channels, leading to HCN formation, are considered. While reactions involving the CN  
33  
34 radical may produce both cyano- and isocyano- compounds, only the former pathways are  
35  
36 considered in these calculations. Previous work on the CN + benzene reaction<sup>34</sup> showed a  
37  
38 significant barrier ( $28 \text{ kJ mol}^{-1}$ ) to isocyano products, which suggests that this pathway will not be  
39  
40 relevant in the ISM.  
41  
42  
43  
44  
45  
46  
47  
48  
49  
50  
51  
52  
53  
54  
55  
56  
57  
58  
59  
60



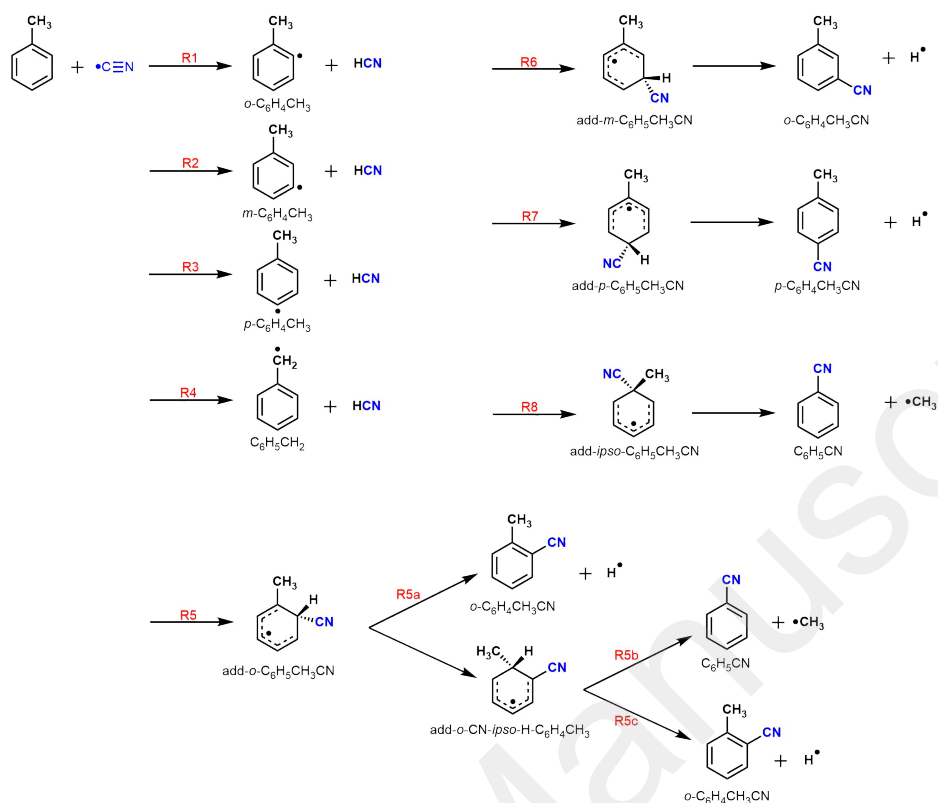


**Figure 1:** The reaction pathways of the CN + toluene reaction and possible products of the abstraction (R1-R4) and CN-addition (R5-R8) channels that are considered in the theoretical calculations.

## Results

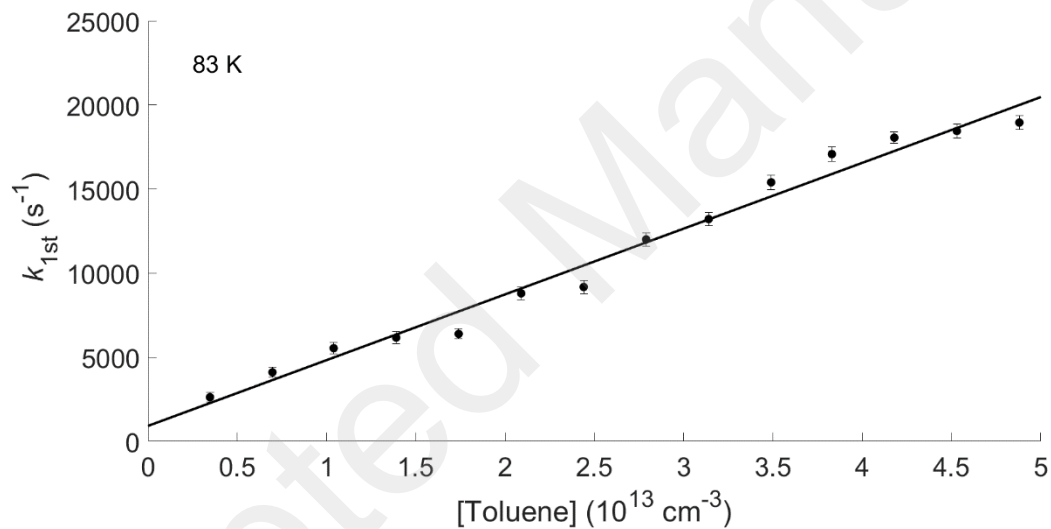
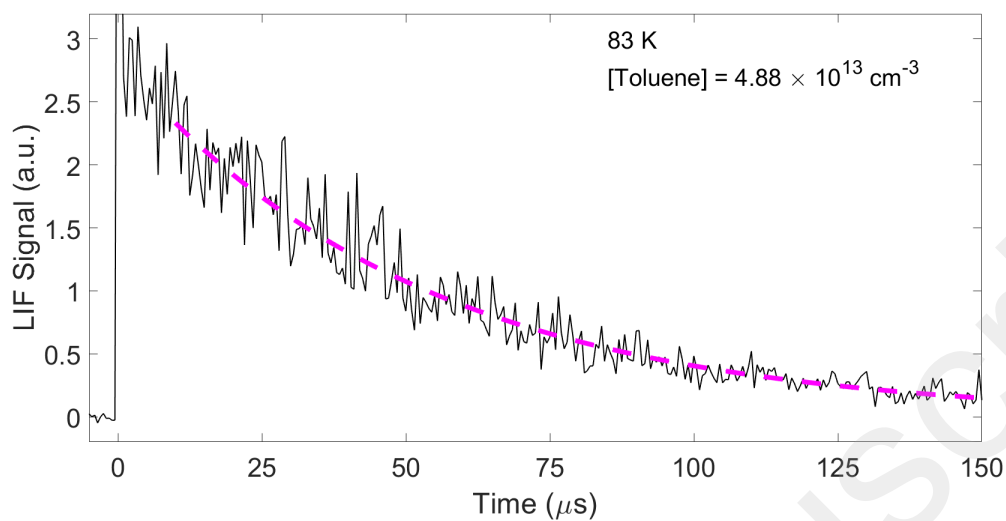


**Figure 2:** Typical experimental kinetics of the CN radical measured using PLP-LIF, showing the decay of the CN signal and resulting second-order plot at 83 K.

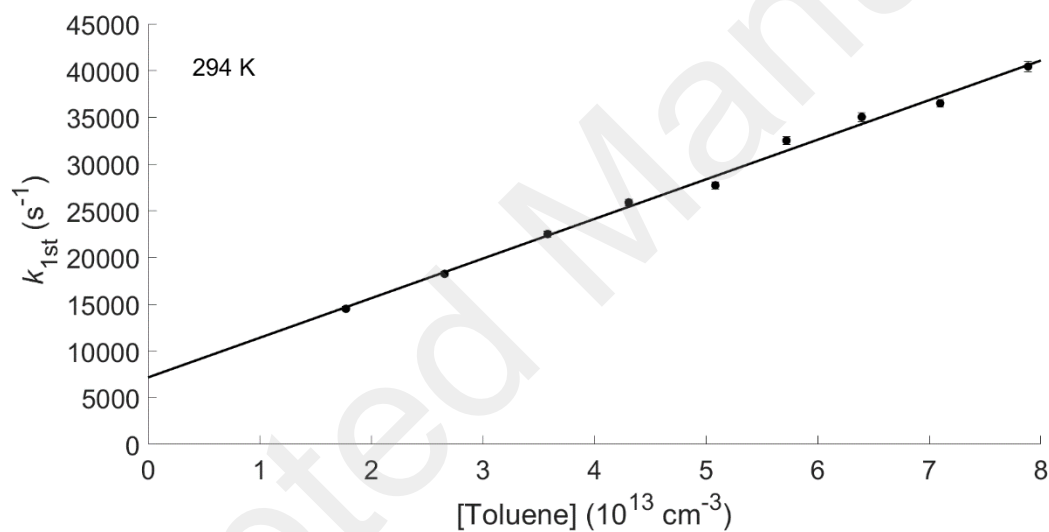
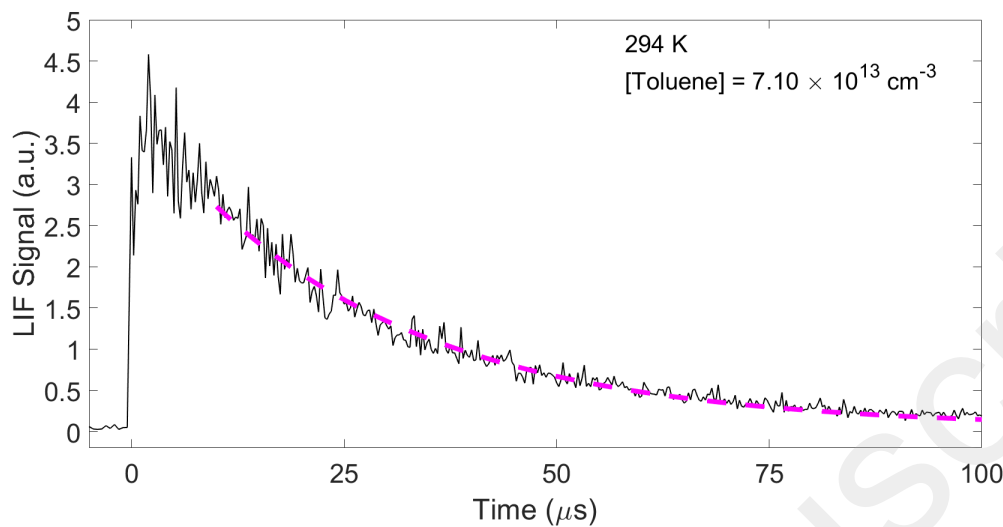


**Figure 3:** Typical experimental kinetics of the CN radical measured using PLP-LIF, showing the decay of the CN signal and resulting second-order plot at 294 K.

Typical LIF decays of CN at 83 K and 294 K and the second-order plots can be seen in Figures 2 and 3, respectively. The non-zero intercepts seen on the second-order plots arise from the loss of CN via side chemistry and diffusion out of the region probed by LIF. From experiments at room temperature, using  $\text{N}_2$  as a buffer gas and varying the total density of the gas flow, we found that

the rate constants had no pressure dependence, implying that the reaction is either a bimolecular reaction, or a termolecular reaction in the high pressure limit in our experimental conditions.

Unlike the room temperature measurements of Trevitt et al., we see no evidence for non-exponential decays at any toluene concentration or total gas density used in these experiments, and the measured rate constants are in good agreement with our values at all other temperatures.

Additional experiments at room temperature demonstrate that changing the buffer gas from N<sub>2</sub> to He does not affect our measured rate constants.

Results of the experiments between 15 and 294 K are shown in Table 1 and Figure 4. At least nine points with varying toluene concentrations were taken for each measurement under pseudo-first order conditions, with toluene in excess. At high reactant concentrations, the formation of toluene dimers causes nonlinear behavior in the second-order plots at the lowest temperatures. This therefore imposes an upper limit on the toluene concentration used in experiments in order to minimize any effect of the reaction between CN and toluene dimers on our measurements.

**Table 1:** Rate coefficients determined for the CN + toluene reaction between 15 and 294 K, along with experimental parameters for each measurement. Uncertainties in the rate constant are the 95% confidence interval from the appropriate Student's *t* test combined in quadrature with a 10% systematic error. Bolded values represent the weighted average and uncertainty for temperatures with multiple measurements.

Temperature (K)	Buffer Gas	Total Density (10 <sup>16</sup> cm <sup>-3</sup> )	[Toluene] (10 <sup>12</sup> cm <sup>-3</sup> )	Number of Points	Rate Constant (10 <sup>-10</sup> cm <sup>3</sup> s <sup>-1</sup> )
15	He	5.04	1.87 – 10.4	10	4.4 ± 0.8
24	He	4.83	1.76 – 19.5	11	4.7 ± 0.6
36	He	5.27	1.25 – 17.7	14	5.9 ± 0.8
36	He	5.32	1.28 – 12.7	9	4.9 ± 1.0
					<b>5.7 ± 0.7</b>
70	He	6.00	2.54 – 15.2	11	4.4 ± 0.7

70	He	6.09	1.34 – 18.7	13	4.2 ± 0.7
					<b>4.3 ± 0.6</b>
83	N <sub>2</sub>	4.63	3.48 – 48.8	14	3.9 ± 0.5
83	N <sub>2</sub>	4.63	1.72 – 31.3	14	3.8 ± 0.4
					<b>3.9 ± 0.4</b>
110	Ar	2.71	1.28 – 14.1	11	3.3 ± 0.5
197	N <sub>2</sub>	5.32	2.13 – 21.4	11	3.7 ± 0.6
294	N <sub>2</sub>	10.5	15.4 – 92.9	11	3.7 ± 0.6
294	N <sub>2</sub>	3.75	9.50 – 47.6	9	4.3 ± 0.6
294	N <sub>2</sub>	8.20	17.7 – 78.9	9	4.3 ± 0.5
294	He	9.41	18.0 – 54.0	11	4.5 ± 0.5
					<b>4.3 ± 0.5</b>

To test whether the photolysis of toluene at 248 nm affected our measurements, we also conducted experiments varying the power of the excimer laser at 110 K, with [Toluene] =  $9 \times 10^{12} \text{ cm}^{-3}$ . We found no significant change in the measured  $k_{1st}$  as a function of our laser power. With the excimer laser fluence of  $25 \text{ mJ cm}^{-2}$  and the toluene absorption cross section at 248 nm of  $2.9 \times 10^{-19} \text{ cm}^2$ ,<sup>35</sup> we expect roughly 1% of the toluene to photolyze if the photolysis quantum yield is 1, which should not measurably affect the observed rate constants. It has also been suggested that two-photon absorption at 248 nm can photolyze toluene to form H atoms among other potential processes,<sup>36</sup> with the total absorption cross section for the second photon experimentally determined to be  $1.7 \times 10^{-17} \text{ cm}^2$ . For the highest toluene concentrations used ( $\sim 1 \times 10^{14} \text{ cm}^{-3}$ ), we estimate at most  $4.8 \times 10^{11} \text{ cm}^{-3}$  of toluene undergoes two-photon absorption, though it is likely much less than that, as discussed in greater detail in the following section, and is unlikely to affect the rate constants measured.

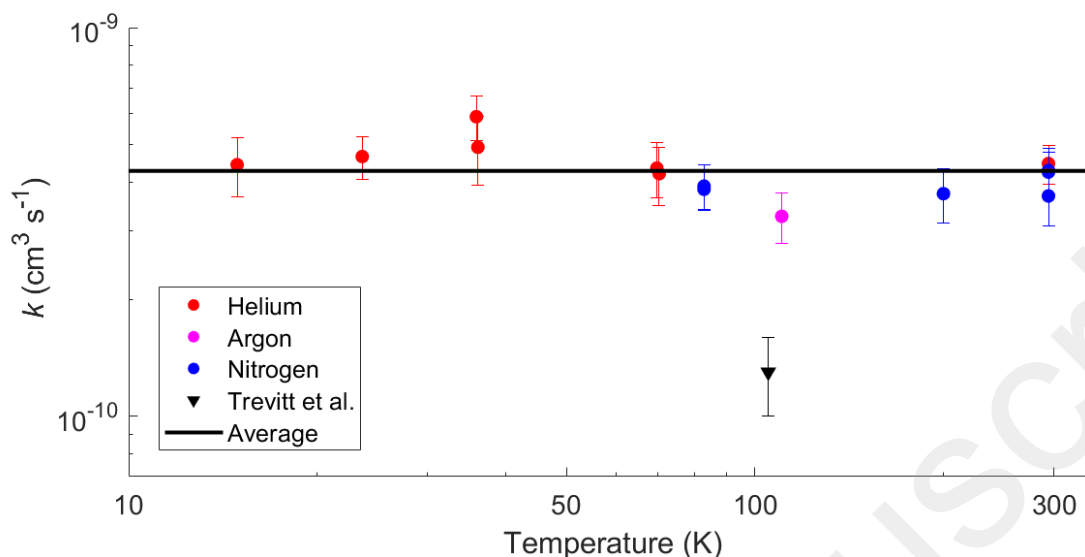


**Figure 4:** The experimental measurements for the CN + toluene rate constant from this work (circles) and Trevitt et al. (triangle); the weighted average value of the measurements presented in this work,  $4.1 \times 10^{-10} \text{ cm}^3 \text{ s}^{-1}$ , is also plotted.

**Table 2:** Zero-point corrected reaction energies and Gibbs energies of the reaction products calculated in this work. Note that some reaction pathways result in the same products.

Reaction channel products	Reaction energy $\Delta_r U^0$ (kcal mol <sup>-1</sup> )	Gibbs energy $\Delta_r G^0$ (298 K) (kcal mol <sup>-1</sup> )
R1 ( <i>o</i> -C <sub>6</sub> H <sub>4</sub> CH <sub>3</sub> + HCN)	-18.1	-18.1
R2 ( <i>m</i> -C <sub>6</sub> H <sub>4</sub> CH <sub>3</sub> + HCN)	-18.3	-18.6
R3 ( <i>p</i> -C <sub>6</sub> H <sub>4</sub> CH <sub>3</sub> + HCN)	-17.8	-18.2
R4 (C <sub>6</sub> H <sub>5</sub> CH <sub>2</sub> + HCN)	-39.1	-38.1
R5a (= R5c, <i>o</i> -C <sub>6</sub> H <sub>4</sub> CH <sub>3</sub> CN + H)	-28.0	-23.6
R5b (= R8, C <sub>6</sub> H <sub>5</sub> CN + CH <sub>3</sub> )	-35.4	-35.5
R5c (= R5a, <i>o</i> -C <sub>6</sub> H <sub>4</sub> CH <sub>3</sub> CN + H)	-28.0	-23.6
R6 ( <i>m</i> -C <sub>6</sub> H <sub>4</sub> CH <sub>3</sub> CN + H)	-26.8	-22.5
R7 ( <i>p</i> -C <sub>6</sub> H <sub>4</sub> CH <sub>3</sub> CN + H)	-27.2	-23.8
R8 (= R5b, C <sub>6</sub> H <sub>5</sub> CN + CH <sub>3</sub> )	-35.4	-35.5

As shown in the Figure 5, both stationary points (reactants, products, intermediates, transition states) for both the abstraction (R1-R4) and addition-elimination (R5-R8) channels were

1  
2  
3 characterized for the reaction between CN and toluene. An additional substitution channel, leading  
4 to the formation of benzyl cyanide, was found to be exothermic at (U)M06-2X/aug-cc-pVTZ, but  
5  
6 has a large barrier ( $\sim 20$  kcal mol<sup>-1</sup>), and hence will not be relevant under interstellar conditions and  
7  
8 is excluded. The relative reaction energy  $\Delta_r U^\circ$  and Gibbs energy at 298 K  $\Delta_r G^\circ$  for all calculated  
9  
10 product channels can be seen in Table 2. Intermediates formed from the addition of CN to the  
11  
12 aromatic ring were found to form barrierlessly, subsequently followed by submerged barriers  
13  
14 leading to the formation of stable nitrile products. This mechanism closely resembles the  
15  
16 mechanism of benzonitrile formation from the reaction of benzene and CN,<sup>34,37</sup> although it does  
17  
18 differ from the reaction between toluene and OH, which features both pre-reactive complexes and  
19  
20 barriers before formation of the addition product.<sup>38</sup> The energies determined for the addition-  
21  
22 elimination channels are generally similar to those calculated for the CN + benzene reaction done  
23  
24 at G3//B3LYP and BCCSD(T)//B3LYP.<sup>34</sup>

25  
26  
27  
28  
29  
30  
31 Abstraction pathways, shown in blue in Figure 5, were found to have slightly submerged transition  
32  
33 states, and therefore are possible products at low temperatures. However, higher level calculations  
34  
35 are needed to confirm these barrier values, as similar abstraction pathways from aromatic  
36  
37 compounds have been shown to possess positive barriers<sup>37-38</sup>. At the level of theory used, these  
38  
39 barrier values are likely within the error of the calculations. An important point to note is that no  
40  
41 transition state or complex could be characterized for the abstraction channels, though we do not  
42  
43 rule out the existence of these stationary points.  
44  
45  
46  
47  
48  
49  
50  
51  
52  
53  
54  
55  
56  
57  
58  
59  
60

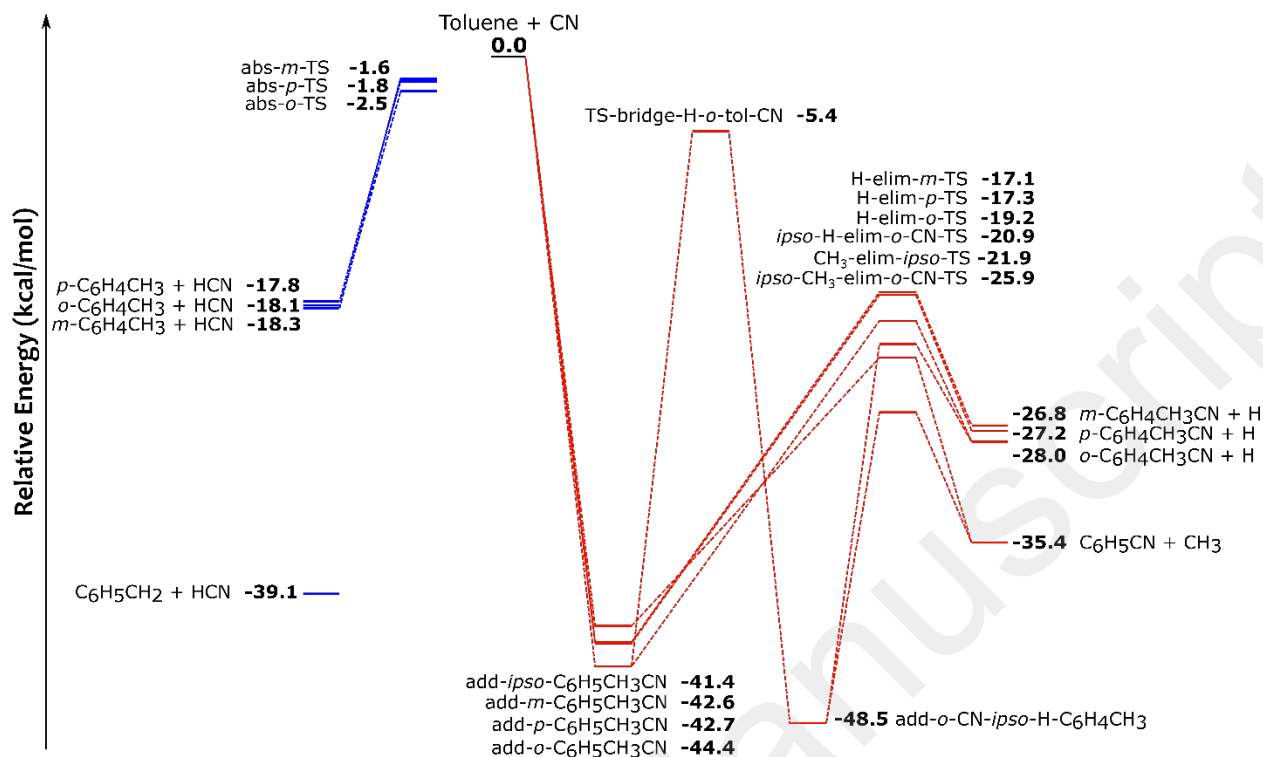


**Figure 5:** The stationary points for PES for the CN + toluene reaction, performed at (U)M06-2X/aug-cc-pVTZ including zero-point energy corrections, showing the abstraction (abs-) pathways (blue) and addition-elimination (add- and elim-) pathways (red), the latter of which can undergo an internal hydrogen shift (-bridge). Note that neither a barrier leading to the formation of  $\text{C}_6\text{H}_5\text{CH}_2 + \text{HCN}$  nor any pre-reactive complexes for the abstraction pathways are included, though we do not preclude their existence.

## Discussion

As Figure 4 demonstrates, we find that the rate constant of the CN + toluene reaction is independent of temperature over the 15 – 294 K range, with a weighted average value of  $(4.1 \pm 0.2) \times 10^{-10} \text{ cm}^3 \text{ s}^{-1}$ . Our results are in contrast to the results of Trevitt et al., who measured a rate constant of  $(1.3 \pm 0.3) \times 10^{-10} \text{ cm}^3 \text{ s}^{-1}$  at 105 K in their LIF experiments. They used a similar LIF method to detect CN, under similar experimental conditions of total density, and CN and toluene concentrations.



1  
2  
3 Furthermore, this group measured CN + benzene rate constants that agree well with recent results  
4  
5 from our group,<sup>23</sup> which suggests that this discrepancy is related to the toluene system.  
6  
7

8 Trevitt et al. reported observing non-exponential decays of CN at room temperature, which they  
9 suggested might be due to back-dissociation of adduct complexes. However, no such behavior was  
10 observed in this work, suggesting that the discrepancy might have arisen from differences in the  
11 photolysis step. Trevitt et al. photolyzed their sample at a wavelength of 266 nm, with a laser  
12 fluence of 40 mJ cm<sup>-2</sup> ( $5.0 \times 10^{16}$  photons cm<sup>-2</sup>, in a probable 3-6 ns long pulse), in contrast to the  
13 248 nm laser beam with a fluence of 25 mJ cm<sup>-2</sup> ( $3.1 \times 10^{16}$  photons cm<sup>-2</sup>, 22 ns long pulse) used  
14 in this work. The ICN photolysis cross sections are similar at these two wavelengths.<sup>28,39</sup> At room  
15 temperature, the toluene absorption cross section to the S<sub>1</sub> state at 266 nm is  $1.3 \times 10^{-19}$  cm<sup>2</sup>.<sup>40</sup> The  
16 S<sub>1</sub> state fluoresces with a lifetime of 86 ns when excited at 266 nm at low pressures.<sup>41</sup> At 248 nm,  
17 the cross section is larger ( $2.9 \times 10^{-19}$  cm<sup>2</sup>)<sup>40</sup> but the fluorescence lifetime is much shorter due to  
18 rapid internal conversion to S<sub>0</sub>, displaying approximately equal intensity 3 ns and 26 ns  
19 components at low pressures.<sup>42</sup> As discussed above, multiphoton absorption at 248 nm of toluene  
20 is known to lead to photolysis,<sup>36</sup> and may additionally lead to photoionization, as the excited  
21 toluene is higher in energy than the ionization onset of toluene (8.3 eV).<sup>43</sup> Both of these processes  
22 are also likely to occur in the 266 nm experiments.  
23  
24  
25  
26  
27  
28  
29  
30  
31  
32  
33  
34  
35  
36  
37  
38  
39  
40  
41  
42  
43

44 The above considerations suggest that single photon excitation of toluene is occurring at both  
45 photolysis wavelengths, but only multiphoton effects are likely to give rise to interferences.  
46  
47 Possible pathways for CN generation on the timescale of the experiment exist by either two-photon  
48 photodissociation or two-photon ionization, particularly at 266 nm by quadrupled Nd:YAG lasers.  
49  
50  
51  
52  
53  
54 Such effects are likely to be significantly lower when toluene is excited at 248 nm light produced  
55  
56  
57  
58  
59  
60

1  
2  
3 by an excimer, due to the longer pulse duration and rapid internal conversion of the  $S_1$  state. This  
4 is in good agreement with the experimental measurements reported here, showing no relationship  
5 between excimer power and  $k_{1st}$ , and no evidence for non-exponential decays. In the experiments  
6 of Trevitt et al. at 266 nm, however, the long lifetime of the  $S_1$  state, short photolysis pulse duration  
7 and higher laser fluence may have caused larger amounts of multi-photon absorption to occur,  
8 such that photodissociation or photoionization products could have affected their measurements  
9 for toluene. Such effects would not be observed upon 266 nm excitation of benzene, however, as  
10 266 nm lies below the absorption threshold for the benzene  $S_1$  state and so two-photon dissociation  
11 would have to occur by a non-resonant process.  
12  
13  
14  
15  
16  
17  
18  
19  
20  
21  
22  
23

24 Further work from Trevitt et al. measured branching ratios at room temperature, using slow flow  
25 reactors in conjunction with product detection by multiplexed photoionization mass spectrometry  
26 (MPIMS) to identify species by mass and photoionization spectrum. They found that the reaction  
27 between CN and toluene exclusively forms tolunitrile (methylbenzotrile), with no evidence for  
28 the hydrogen abstraction channels or for benzonitrile formation. Due to the similarities in the  
29 calculated photoionization spectra of the *ortho*-, *meta*-, and *para*- isomers of the tolunitrile, they  
30 were unable to distinguish the precise isomers of tolunitrile formed from this reaction. They found  
31 a similar result for the reaction of CN with benzene, with benzonitrile being the only detected  
32 product. Lenis and Miller also measured the products of the CN + toluene reaction using the 254  
33 nm photolysis of ICN and analyzing the resulting products with GC-MS<sup>44</sup> and observed both  
34 tolunitrile and a small yield (9%) of benzonitrile. While it is unclear if this benzonitrile is formed  
35 as a result of CN + toluene or side chemistry, particularly in light of its non-detection in the MPIMS  
36 experiments by Trevitt et al., our calculations do show potential pathways to benzonitrile formation  
37 from *ortho*- or *ipso*- addition of CN to the aromatic ring.  
38  
39  
40  
41  
42  
43  
44  
45  
46  
47  
48  
49  
50  
51  
52  
53  
54  
55  
56  
57  
58  
59  
60

1  
2  
3 The rate constants measured here are in good agreement with the value of  $(4.4 \pm 0.2) \times 10^{-10} \text{ cm}^3$   
4  $\text{s}^{-1}$ , independent of temperature over 15 – 295 K range, that we determined for the reaction between  
5  
6 CN and benzene.<sup>23</sup> In conjunction with the similarities in products measured by MPIMS, this  
7  
8 suggests that the major mechanism is the same for reactions between the CN radical and either  
9  
10 benzene or toluene, and results in formation of cyano-substituted aromatic compounds.  
11  
12 Investigation of other substituted compounds, such as xylenes or deuterium-substituted benzene,  
13  
14 may yield further insight into whether this mechanism is general for these reactions. This will aid  
15  
16 in future astronomical searches to improve our understanding of the formation of small aromatic  
17  
18 rings in the ISM.  
19  
20  
21  
22  
23

24  
25 The submerged barriers found for the various channels using quantum chemical calculations  
26  
27 highlight the diversity of the products that could be formed from this reaction at low temperatures.  
28  
29 While the abstraction channels were found to have slightly submerged barriers, calculations at  
30  
31 higher level of theory are necessary to correctly estimate their energies. Furthermore, the transition  
32  
33 state(s) and/or a possible complex in the case of the hydrogen abstraction from the methyl group  
34  
35 pathway remain to be explored further. This will also provide the accuracy necessary for master  
36  
37 equation calculations, which would further elucidate the mechanism and product branching ratios  
38  
39 of this reaction.  
40  
41  
42  
43

44 On Titan, the CN radical is mainly generated from the photolysis of HCN, which is formed through  
45  
46 reactions of  $\text{N}(^4\text{S})$  or through ion chemistry.<sup>4-5</sup> Once formed, CN reacts primarily with the highly  
47  
48 abundant  $\text{CH}_4$  to reform HCN. This cycle can be interrupted, however, by CN reactions with other  
49  
50 compounds, most commonly  $\text{C}_2\text{H}_2$  or  $\text{HC}_3\text{N}$ . While this reaction has not explicitly been included  
51  
52 in models, recent work has suggested that the concentrations of benzene and toluene in the Titan  
53  
54 atmosphere are similar, peaking at a mole fraction of  $10^{-6}$  at an altitude of roughly 1000 km above  
55  
56  
57  
58  
59  
60

1  
2  
3 the surface.<sup>11</sup> Benzonitrile has not been detected on Titan and is predicted to be formed in low  
4 quantities, largely due to CN being sequestered by reaction with CH<sub>4</sub>. Even with the larger rate  
5 constants measured in this work, this is likely also the case for the products of the reaction between  
6 CN and toluene, though implementation of these results into Titan models may still be beneficial  
7 to determine if they have any influence in the atmosphere.  
8  
9

10  
11  
12  
13  
14  
15 Astronomical searches for toluene and the tolunitrile products of this reaction would test the  
16 robustness of using cyano-containing species as proxies for the unsubstituted hydrocarbons. While  
17 benzene has no permanent dipole moment, toluene has a small one (0.37 Debye)<sup>45</sup> and may be  
18 observable via radio astronomy, though it would have to be present in higher abundance than, say  
19 benzonitrile, to be detectable. The use of velocity stacking, which averages the signal of multiple  
20 transitions together to increase the signal-to-noise ratio,<sup>46-48</sup> may assist in searching for toluene in  
21 the ISM. While there have been no previous detections of toluene in the ISM, it has been argued  
22 that the protonated toluene ion, C<sub>7</sub>H<sub>9</sub><sup>+</sup>,<sup>49</sup> and methyl-substituted PAHs<sup>50-51</sup> are possible carriers of  
23 the 6.2 and the 3.4 μm unidentified infrared bands, respectively. Definitive detection of toluene  
24 and related compounds, such as these, would allow us to constrain aromatic pathways and, in  
25 particular, could test the bottom-up mechanism for PAH formation, wherein small molecules, such  
26 as toluene, react progressively to form large clusters.  
27  
28  
29  
30  
31  
32  
33  
34  
35  
36  
37  
38  
39  
40  
41  
42  
43

44 The origin of the first aromatic ring in the interstellar medium in molecules such as benzene and  
45 toluene remains unknown. It has been argued that the reaction between C<sub>2</sub>H and isoprene (C<sub>5</sub>H<sub>8</sub>;  
46 2-methyl-1,3-butadiene), a barrierless reaction that produces toluene, may be a source of it at low  
47 temperatures,<sup>52</sup> but it is unknown whether isoprene is present in the ISM – isoprene is not included  
48 in astrochemical databases such as the Kinetic Database for Astrochemistry<sup>53</sup> (kida.obs.u-  
49  
50  
51  
52  
53  
54  
55  
56  
57  
58  
59  
60

1  
2  
3 bordeaux1.fr, accessed July 2020). Other mechanisms, such as ion-neutral reactions, may also  
4  
5 contribute, but further investigation is necessary.  
6  
7

8  
9 In order to better understand the potential formation pathways of these products of this reaction in  
10  
11 the ISM, more accurate measurements of the product ratios are required, and specifically, the  
12  
13 branching ratio for the tolunitrile and potential benzonitrile products. While challenging for many  
14  
15 techniques due to the similarities of the isomers, recent work has coupled low temperature  
16  
17 supersonic uniform flows to microwave spectrometers<sup>54-55</sup> in order to determine branching ratios  
18  
19 relevant for astrochemistry. As each of these compounds will have a unique rotational spectrum,  
20  
21 this technique is well suited for quantitatively measuring the product branching ratio of this  
22  
23 reaction.  
24  
25

## 26 27 28 **Conclusions**

29  
30  
31 We have measured rate constants for the CN + toluene reaction between 15 and 294 K and find  
32  
33 that the rate constant is independent of temperature over this range. These results closely match  
34  
35 our recent study on the reaction of CN with benzene but are higher than the only previous  
36  
37 measurement of this rate constant at 105 K, for reasons that remain unresolved, but may be related  
38  
39 to multiphoton effects at the higher laser intensities and 266 nm photolysis wavelength used in that  
40  
41 study. This similarly suggests that the reactions between CN and simple aromatics proceed through  
42  
43 an analogous mechanism, which is supported by our theoretical calculations and previous product  
44  
45 measurements. Further work, particularly on the products formed from this reaction, would be  
46  
47 beneficial to determine their potential detectability in the ISM. The ability to detect and use cyano-  
48  
49 substituted aromatics, which have large dipole moments, as proxies for unsubstituted aromatic  
50  
51 compounds in the ISM would help advance our knowledge of PAH formation.  
52  
53  
54  
55  
56  
57  
58  
59  
60

## Supporting Information

Geometries of calculated structures for all molecules and transition states

## Acknowledgments

The authors thank Jonathan Courbe, Jonathan Thiévin, Didier Biet, Ewen Gallou and Alexandre Dapp for technical support. We would like to acknowledge Mayank Saraswat for helpful discussions regarding the PES calculations. J. P. M. was supported by the National Science Foundation Graduate Research Fellowship (NSF GRP) and the National Science Foundation Graduate Research Opportunities Worldwide (NSF GROW) programs. J. P. M. would also like to thank the Office of Science and Technology of the Embassy of France in the United States for a Chateaubriand Fellowship. The authors acknowledge funding from the European Union's Horizon 2020 research and innovation programme under the European Research Council (ERC) grant agreement 695724-CRESUCHIRP and under the Marie Skłodowska-Curie grant agreement 845165-MIRAGE. Acknowledgment is made to the donors of The American Chemical Society Petroleum Research Fund for partial support of this research. The authors are also grateful for support from the European Regional Development Fund, the Region of Brittany and Rennes Metropole. This work was supported by the French National Programme "Physique et Chimie du Milieu Interstellaire" (PCMI) of CNRS/INSU with INC/INP co-funded by CEA and CNES.

## References

1. Adams, W. S., Some Results with the Coude Spectrograph of the Mount Wilson Observatory. *Astrophys J* **1941**, *93*, 11-23.
2. McKellar, A., Evidence for the Molecular Origin of Some Hitherto Unidentified Interstellar Lines. *Publ Astron Soc Pacc* **1940**, *52*, 187 - 192.
3. Yung, Y. L.; Allen, M.; Pinto, J. P., Photochemistry of the Atmosphere of Titan - Comparison between Model and Observations. *Astrophys J Suppl S* **1984**, *55*, 465-506.

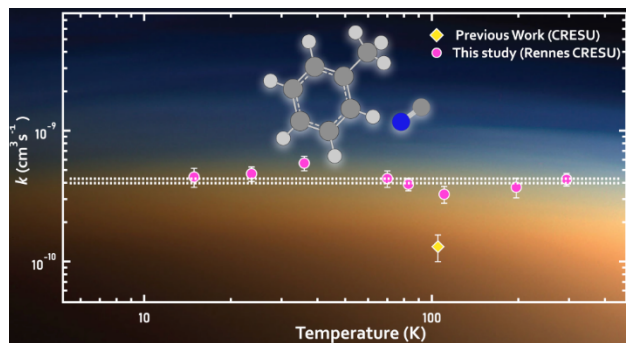
4. Loison, J. C.; Hebrard, E.; Dobrijevic, M.; Hickson, K. M.; Caralp, F.; Hue, V.; Gronoff, G.; Venot, O.; Benilan, Y., The Neutral Photochemistry of Nitriles, Amines and Imines in the Atmosphere of Titan. *Icarus* **2015**, *247*, 218-247.
5. Wilson, E. H.; Atreya, S. K., Current State of Modeling the Photochemistry of Titan's Mutually Dependent Atmosphere and Ionosphere. *J Geophys Res* **2004**, *109*, E06002.
6. Cooke, I. R.; Sims, I. R., Experimental Studies of Gas-Phase Reactivity in Relation to Complex Organic Molecules in Star-Forming Regions. *ACS Earth Space Chem* **2019**, *3*, 1109-1134.
7. Broten, N. W.; Oka, T.; Avery, L. W.; Macleod, J. M.; Kroto, H. W., The Detection of HC9N in Interstellar Space. *Astrophys J* **1978**, *223*, L105-L107.
8. Belloche, A.; Garrod, R. T.; Muller, H. S. P.; Menten, K. M., Detection of a Branched Alkyl Molecule in the Interstellar Medium: Iso-Propyl Cyanide. *Science* **2014**, *345*, 1584-1587.
9. Gudipati, M. S.; Jacovi, R.; Couturier-Tamburelli, I.; Lignell, A.; Allen, M., Photochemical Activity of Titan's Low-Altitude Condensed Haze. *Nat Commun* **2013**, *4*, 1648.
10. Magee, B. A.; Waite, J. H.; Mandt, K. E.; Westlake, J.; Bell, J.; Gell, D. A., INMS-Derived Composition of Titan's Upper Atmosphere: Analysis Methods and Model Comparison. *Planet Space Sci* **2009**, *57*, 1895-1916.
11. Loison, J. C.; Dobrijevic, M.; Hickson, K. M., The Photochemical Production of Aromatics in the Atmosphere of Titan. *Icarus* **2019**, *329*, 55-71.
12. Lopez-Puertas, M.; Dinelli, B. M.; Adriani, A.; Funke, B.; Garcia-Comas, M.; Moriconi, M. L.; D'Aversa, E.; Boersma, C.; Allamandola, L. J., Large Abundances of Polycyclic Aromatic Hydrocarbons in Titan's Upper Atmosphere. *Astrophys J* **2013**, *770*.
13. Wilson, E. H.; Atreya, S. K., Chemical Sources of Haze Formation in Titan's Atmosphere. *Planet Space Sci* **2003**, *51*, 1017-1033.
14. Cernicharo, J.; Heras, A. M.; Tielens, A. G. G. M.; Pardo, J. R.; Herpin, F.; Guelin, M.; Waters, L. B. F. M., Infrared Space Observatory's Discovery of C<sub>4</sub>H<sub>2</sub>, C<sub>6</sub>H<sub>2</sub>, and Benzene in CRL 618. *Astrophys J* **2001**, *546*, L123-L126.
15. Lovas, F. J.; McMahon, R. J.; Grabow, J. U.; Schnell, M.; Mack, J.; Scott, L. T.; Kuczkowski, R. L., Interstellar Chemistry: A Strategy for Detecting Polycyclic Aromatic Hydrocarbons in Space. *J Am Chem Soc* **2005**, *127*, 4345-4349.
16. Chiar, J. E.; Tielens, A. G. G. M.; Adamson, A. J.; Ricca, A., The Structure, Origin, and Evolution of Interstellar Hydrocarbon Grains. *Astrophys J* **2013**, *770*.
17. Dwek, E., et al., Detection and Characterization of Cold Interstellar Dust and Polycyclic Aromatic Hydrocarbon Emission, from COBE Observations. *Astrophys J* **1997**, *475*, 565-579.
18. Wakelam, V.; Herbst, E., Polycyclic Aromatic Hydrocarbons in Dense Cloud Chemistry. *Astrophys J* **2008**, *680*, 371-383.
19. Kaiser, R. I.; Parker, D. S. N.; Mebel, A. M., Reaction Dynamics in Astrochemistry: Low-Temperature Pathways to Polycyclic Aromatic Hydrocarbons in the Interstellar Medium. *Annu Rev Phys Chem, Vol 66* **2015**, *66*, 43-67.
20. Tielens, A. G. G. M., Interstellar Polycyclic Aromatic Hydrocarbon Molecules. *Annu Rev Astron Astr* **2008**, *46*, 289-337.
21. Tielens, A. G. G. M.; Charnley, S. B., Circumstellar and Interstellar Synthesis of Organic Molecules. *Origins Life Evol B* **1997**, *27*, 23-51.
22. McGuire, B. A.; Burkhardt, A. M.; Kalenskii, S.; Shingledecker, C. N.; Remijan, A. J.; Herbst, E.; McCarthy, M. C., Detection of the Aromatic Molecule Benzonitrile (C-C<sub>6</sub>H<sub>5</sub>CN) in the Interstellar Medium. *Science* **2018**, *359*, 202-205.

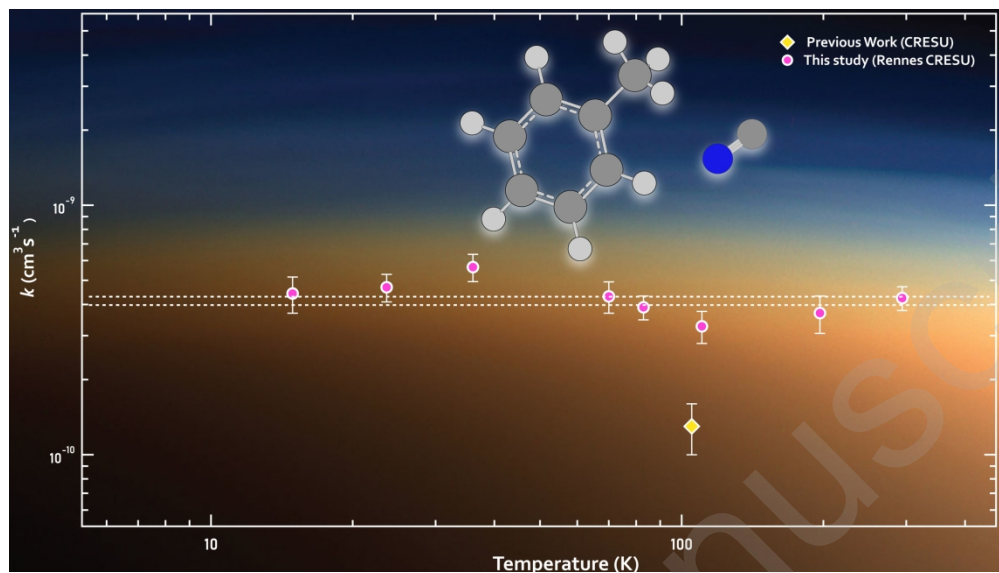
23. Cooke, I. R.; Gupta, D.; Messinger, J. P.; Sims, I. R., Benzonitrile as a Proxy for Benzene in the Cold Ism: Low-Temperature Rate Coefficients for CN + C<sub>6</sub>H<sub>6</sub>. *Astrophys J Lett* **2020**, *891*.
24. Trevitt, A. J.; Goulay, F.; Taatjes, C. A.; Osborn, D. L.; Leone, S. R., Reactions of the CN Radical with Benzene and Toluene: Product Detection and Low-Temperature Kinetics. *J Phys Chem A* **2010**, *114*, 1749-1755.
25. James, P. L.; Sims, I. R.; Smith, I. W. M.; Alexander, M. H.; Yang, M. B., A Combined Experimental and Theoretical Study of Rotational Energy Transfer in Collisions between NO(X (2)Pi(1/2), V=3,J) and He, Ar and N<sub>2</sub> at Temperatures Down to 7 K. *J Chem Phys* **1998**, *109*, 3882-3897.
26. Sims, I. R.; Queffelec, J. L.; Defrance, A.; Rebrionrowe, C.; Travers, D.; Bocherel, P.; Rowe, B. R.; Smith, I. W. M., Ultralow Temperature Kinetics of Neutral-Neutral Reactions - the Technique and Results for the Reactions CN+O<sub>2</sub> Down to 13 K and CN+NH<sub>3</sub> Down to 25 K. *J Chem Phys* **1994**, *100*, 4229-4241.
27. Gupta, D.; Ely, S. C. S.; Cooke, I. R.; Guillaume, T.; Khedaoui, O. A.; Hearne, T. S.; Hays, B. M.; Sims, I. R., Low Temperature Kinetics of the Reaction between Methanol and the CN Radical. *J Phys Chem A* **2019**, *123*, 9995-10003.
28. Felps, W. S.; Rupnik, K.; Mcglynn, S. P., Electronic Spectroscopy of the Cyanogen Halides. *J Phys Chem* **1991**, *95*, 639-656.
29. O'Halloran, M. A.; Joswig, H.; Zare, R. N., Alignment of CN from 248 nm Photolysis of ICN - a New Model of the a Continuum Dissociation Dynamics. *J Chem Phys* **1987**, *87*, 303-313.
30. Frisch, M. J., et al. *Gaussian 09*, Gaussian, Inc.: Wallingford, CT, USA, 2009.
31. Kendall, R. A.; Dunning, T. H.; Harrison, R. J., Electron-Affinities of the 1st-Row Atoms Revisited - Systematic Basis-Sets and Wave-Functions. *J Chem Phys* **1992**, *96*, 6796-6806.
32. Woon, D. E.; Dunning, T. H., Gaussian-Basis Sets for Use in Correlated Molecular Calculations 3. The Atoms Aluminum through Argon. *J Chem Phys* **1993**, *98*, 1358-1371.
33. Zhao, Y.; Truhlar, D. G., The M06 Suite of Density Functionals for Main Group Thermochemistry, Thermochemical Kinetics, Noncovalent Interactions, Excited States, and Transition Elements: Two New Functionals and Systematic Testing of Four M06-Class Functionals and 12 Other Functionals. *Theor Chem Acc* **2008**, *120*, 215-241.
34. Lee, K. L. K.; McGuire, B. A.; McCarthy, M. C., Gas-Phase Synthetic Pathways to Benzene and Benzonitrile: A Combined Microwave and Thermochemical Investigation. *Phys Chem Chem Phys* **2019**, *21*, 2946-2956.
35. Koban, W.; Koch, J. D.; Hanson, R. K.; Schulz, C., Absorption and Fluorescence of Toluene Vapor at Elevated Temperatures. *Phys Chem Chem Phys* **2004**, *6*, 2940-2945.
36. Kovacs, T.; Blitz, M. A.; Seakins, P. W.; Pilling, M. J., H Atom Formation from Benzene and Toluene Photoexcitation at 248 nm. *J Chem Phys* **2009**, *131*.
37. Woon, D. E., Modeling Chemical Growth Processes in Titan's Atmosphere: 1. Theoretical Rates for Reactions between Benzene and the Ethynyl (C<sub>2</sub>H) and Cyano (CN) Radicals at Low Temperature and Pressure. *Chem Phys* **2006**, *331*, 67-76.
38. Zhang, R. M.; Truhlar, D. G.; Xu, X. F., Kinetics of the Toluene Reaction with OH Radical. *Research-China* **2019**, *2019*.
39. Myer, J. A.; Samson, J. A. R., Vacuum-Ultraviolet Absorption Cross Sections of CO, HCl, and ICN between 1050 and 2100 Å. *J Chem Phys* **1970**, *52*, 266-&.



- 1  
2  
3  
4  
5  
6  
7  
8  
9  
10  
11  
12  
13  
14  
15  
16  
17  
18  
19  
20  
21  
22  
23  
24  
25  
26  
27  
28  
29  
30  
31  
32  
33  
34  
35  
36  
37  
38  
39  
40  
41  
42  
43  
44  
45  
46  
47  
48  
49  
50  
51  
52  
53  
54
40. Fally, S.; Carleer, M.; Vandaele, A. C., UV Fourier Transform Absorption Cross Sections of Benzene, Toluene, Meta-, Ortho-, and Para-Xylene. *J Quant Spectrosc Ra* **2009**, *110*, 766-782.
  41. Hickman, C. G.; Gascooke, J. R.; Lawrance, W. D., The S1-S0(1b2-1a1) Transition of Jet-Cooled Toluene: Excitation and Dispersed Fluorescence Spectra, Fluorescence Lifetimes, and Intramolecular Vibrational Energy Redistribution. *J Chem Phys* **1996**, *104*, 4887-4901.
  42. Jacon, M.; Lardeux, C.; Lopez-Delgado, R.; Tramer, A. On the “third decay channel” and vibrational redistribution problems in benzene derivatives. *Chem Phys* **1977**, *24*, 145-157.
  43. Lu, K. T.; Eiden, G. C.; Weisshaar, J. C., Toluene Cation - Nearly Free Rotation of the Methyl-Group. *J Phys Chem* **1992**, *96*, 9742-9748.
  44. Henis, N. B. H.; Miller, L. L., Mechanism of Gas-Phase Cyanation of Alkenes and Aromatics. *J Am Chem Soc* **1983**, *105*, 2820-2823.
  45. Rudolph, H. D.; Dreizler, H.; Jaeschke, A.; Wendling, P., Mikrowellenspektrum Hinderungspotential Der Internen Rotation Und Dipolmoment Des Toluols. *Z Naturforsch Pt A* **1967**, *A 22*, 940-&.
  46. Loomis, R. A., et al., Non-Detection of Hc11n Towards Tmc-1: Constraining the Chemistry of Large Carbon-Chain Molecules. *Mon Not R Astron Soc* **2016**, *463*, 4175-4183.
  47. Walsh, C.; Loomis, R. A.; Oberg, K. I.; Kama, M.; van't Hoff, M. L. R.; Millar, T. J.; Aikawa, Y.; Herbst, E.; Weaver, S. L. W.; Nomura, H., First Detection of Gas-Phase Methanol in a Protoplanetary Disk. *Astrophys J Lett* **2016**, 823.
  48. Langston, G.; Turner, B., Detection of <sup>13</sup>C Isotopomers of the Molecule HC7N. *Astrophys J* **2007**, *658*, 455-461.
  49. Douberly, G. E.; Ricks, A. M.; Schleyer, P. V. R.; Duncan, M. A., Infrared Spectroscopy of Gas Phase Benzenium Ions: Protonated Benzene and Protonated Toluene, from 750 to 3400 cm<sup>-1</sup>. *J Phys Chem A* **2008**, *112*, 4869-4874.
  50. Joblin, C.; Tielens, A. G. G. M.; Allamandola, L. J.; Geballe, T. R., Spatial Variation of the 3.29 and 3.40 Micron Emission Bands within Reflection Nebulae and the Photochemical Evolution of Methylated Polycyclic Aromatic Hydrocarbons. *Astrophys J* **1996**, *458*, 610-620.
  51. Wagner, D. R.; Kim, H. S.; Saykally, R. J., Peripherally Hydrogenated Neutral Polycyclic Aromatic Hydrocarbons as Carriers of the 3 Micron Interstellar Infrared Emission Complex: Results from Single-Photon Infrared Emission Spectroscopy. *Astrophys J* **2000**, *545*, 854-860.
  52. Dangi, B. B.; Parker, D. S.; Kaiser, R. I.; Jamal, A.; Mebel, A. M., A Combined Experimental and Theoretical Study on the Gas-Phase Synthesis of Toluene under Single Collision Conditions. *Angew Chem Int Ed Engl* **2013**, *52*, 7186-9.
  53. Wakelam, V., et al., A Kinetic Database for Astrochemistry (KIDA). *Astrophys J Suppl S* **2012**, 199.
  54. Abeysekera, C.; Joalland, B.; Ariyasingha, N.; Zack, L. N.; Sims, I. R.; Field, R. W.; Suits, A. G., Product Branching in the Low Temperature Reaction of CN with Propyne by Chirped-Pulse Microwave Spectroscopy in a Uniform Supersonic Flow. *J Phys Chem Lett* **2015**, *6*, 1599-1604.
  55. Hays, B. M.; Guillaume, T.; Hearne, T. S.; Cooke, I. R.; Gupta, D.; Abdelkdaer Khedaoui, O.; Le Picard, S. D.; Sims, I. R., Design and Performance of an E-Band Chirped Pulse Spectrometer for Kinetics Applications: OCS - He Pressure Broadening. *J Quant Spectrosc Ra* **2020**, 250.

## TOC Image





TOC image

677x381mm (96 x 96 DPI)